Noname manuscript No.
(will be inserted by the editor)

A calibration-free approach to implementing P300-based brain-computer interface

Zhihua Huang · Jiannan Guo · Wenming Zheng · Yingjie Wu · Zhixiong Lin · Huiru Zheng

Received: date / Accepted: date

Abstract Introduction: As a direct bridge between the brain and the outer world, brain-computer interface (BCI) is expected to replace, restore, enhance, supplement, or improve the natural output of brain. The prospect of BCI serving humans is very broad. However, the extensive applications of BCI have not been fully achieved. One of reasons is that the cost of calibration reduces the convenience and usability of BCI. Methods: In this study, we proposed a calibration-free approach, which is based on the ideas of reinforcement learning and transfer learning, for P300-based BCI. This approach, composed of two algorithms: P300 linear upper confidence bound (PLUCB) and transferred PLUCB (TPLUCB), is able to learn during the usage by exploration and exploitation and allows P300-based BCI to start working without any calibration. Results: We tested the performances of PLUCB and TPLUCB using stepwise linear discriminant analysis (SWLDA), a commonly-used method that needs calibration, as a baseline in simulated online experiments. The results showed the merits of PLUCB and TPLUCB. PLUCB can quickly increase the accuracies to the level of SWLDA. TPLUCB has surpassed SWLDA in the *sample accuracy* since it starts running. Both PLUCB and TPLUCB have the ability to keep improving the classification performance during the process. The *overall sample accuracies* ($73.6 \pm 4.8\%$, $73.1 \pm 4.9\%$), *overall symbol accuracies* ($80.4 \pm 12.8\%$, $79.6 \pm 14.0\%$), F-measures (0.45 ± 0.06, 0.44 ± 0.06) and information transfer ratios (ITR) (36.4 ± 9.1, 35.5 ± 9.8) of PLUCB and TPLUCB are significantly better than those of SWLDA (*overall sample accuracy*: $58.8 \pm 3.8\%$, *overall symbol accuracy*: $69.0 \pm 18.3\%$, F-measure: 0.38 ± 0.04, ITR: 28.7 ± 10.7). Conclusions: The proposed approach, which doesn't need calibration but outperform SWLDA, is a very good option for the implementation of P300-based BCI.

Keywords P300 BCI · Reinforcement learning · Transfer learning · Calibration-free

Correspondence should be addressed to Zhihua Huang, College of Computer and Data Science, Fuzhou University, Fuzhou 350108, China. E-mail: hzh@fzu.edu.cn (Z.H.); Linzx@ccmu.edu.cn (Z.L.); h.zheng@ulster.ac.uk (H.Z.)

Zhihua Huang
College of Computer and Data Science, Fuzhou University, Fuzhou 350108, China.

Jiannan Guo
College of Computer and Data Science, Fuzhou University, Fuzhou 350108, China.

Wenming Zheng
Key Laboratory of Child Development and Learning Science of Ministry of Education, Research Center for Learning Science, Southeast University, Nanjing 210096, China.

Yingjie Wu
College of Computer and Data Science, Fuzhou University, Fuzhou 350108, China.

Zhixiong Lin
Department of Neurosurgery, Sanbo Brain Hospital of Capital Medical University, Beijing, 100093, China.

Huiru Zheng
School of Computing, Ulster University, United Kingdom.

1 Introduction

Brain-computer interface (BCI) is a direct bridge between the brain and the outer world. BCI can transmit the information of the brain, bypassing the peripheral nervous system and muscle [1]. The exciting advances in the field of BCI have attracted research interests in various applications [1–3]. BCI is expected to replace, restore, enhance, supplement, or improve the natural output of the brain [1, 4, 5]. Since cross-session and cross-subject variabilities exist in electroen-

cephalogram (EEG), the classifier used to detect EEG needs to be trained before every use. Training before every use, which is often called calibration, is very time-consuming. The cost of calibration is one of very important factors hindering the widespread use of BCI [1].

Research has been carried out to reduce the calibration cost of BCI. There are two different approaches. The first one is to transfer knowledge to new users from previous users. The basis of this approach is transfer learning theory [6–9]. By applying transfer learning, very little or even no data is required for calibration when a new user comes in. The second approach is to randomly initiate a classifier and then continuously update it during using BCI. The initial classifiers may perform poorly and the classifiers will adapt to the users through continuous updating. This approach is based on the theory of online learning or reinforcement learning [4, 10–12].

Some studies of applying transfer learning in BCI are described as follows. In 2009, Fazli *et al* [13] reported an attempt to generalize an ensemble of classifiers derived from a large EEG database of motor imagery BCI to new subjects. In 2014, Kindermans *et al* [14] proposed a probabilistic framework with inter-subject transfer learning that could cancel the need of event-related potential (ERP) spelling BCI for calibration. In 2017, Gayraud *et al* [15] applied the optimal transport to develop a method having the potential to cancel the need of P300 speller BCI for calibration. In 2018, Qi *et al* [16] proposed a method to reduce calibration times by using the Riemannian distance measurement to select similar ERP samples. In 2019, Hübner *et al* [17] used learning from label proportions as a new classification approach and proved its value for the visual ERP BCI. In 2020, the investigation of Lee *et al* [18] showed that convolutional neural network (CNN) combined with large ERP samples could achieve calibration-free in a P300 speller BCI. In the same year, the work of Li *et al* [19] demonstrated that the combination of xDAWN spatial filter and Riemannian Geometry Mean can make the data from different subjects comparable, and has the potential to generalize a fixed classification method.

Also, there are some studies on adapting BCI classifiers to users by reinforcement learning or online learning. Early in 2006, Buttfield *et al* [20] presented their investigation of adapting the classifiers to the subjects' EEG by online learning. In 2014, Kindermans *et al* [21] attempted to bypass the calibration recording by utilizing an unsupervised trained classifier, which was initialized randomly and then updated during usage. In the same year, Grizou *et al* [22] proposed a method without the need for calibration, which could continuously update the inference about the interpretation of EEG signals of BCI users as new data comes in. In 2015, Bauer *et al* [4] applied a Bayesian model of neurofeedback and reinforcement learning to study the impact of threshold adaptation of classifiers on optimizing restorative BCIs. In 2018, for emotional state prediction, Liu *et al* [23] proposed a new method that modified the predictor during the online training iterations by exploiting the reward. In 2020, Ma *et al* [24] presented an adaptive projected sub-gradient method whose coefficients are adjusted online as data arrive sequentially. They evaluated its performance through an ERP-based BCI experiment.

Among all types of BCIs, P300-based BCI, proposed by Farwell *et al* [25] in 1988, has been explored in various applications due to its comparative reliability and stability [1, 5]. In this study, we focus on seeking an approach to implementing calibration-free P300-based BCI. According to the fundamental of reinforcement learning [4,10,26,27], we proposed a novel method, P300 linear upper confidence bound [26] (PLUCB), to build P300 predictors for each user without the need of collecting training data. Furthermore, by introducing the idea of transfer learning [6–9], we developed a new version of this method, transferred PLUCB (TPLUCB), which could quickly optimize calibration-free P300-based BCI system for each user based on a pool of predictors.

For P300-based BCI, stepwise linear discriminant analysis (SWLDA) is a commonly-used method [28–31], which needs calibration. Our results show that the calibration-free PLUCB and TPLUCB can achieve comparable accuracies with SWLDA only after undergoing a brief updating and subsequently reach the high points of accuracy that are significantly higher than those of SWLDA. PLUCB and TPLUCB can not only allow starting P300-based BCI without any calibration, but also achieve better performance than SWLDA. They provide a very good option for implementing a P300-based BCI.

Extensive research suggests that bringing together artificial intelligence and cognitive science would benefit both [32]. The proposed approach, which is used to address a BCI issue, originates from the principles of reinforcement learning and transfer learning, which both closely relate to cognitive science [32]. This study, in which artificial intelligence and cognitive science are tightly linked, is a further example of mutual promotion of artificial intelligence and cognitive science.

2 Methods

In the field of neuroscience, reinforcement learning is a cognitive process in which a person utilizes previ-

ous experience to improve his/her strategy. The neural basis of reinforcement learning has been explored in various ways [33, 34]. In the area of machine learning, reinforcement learning, one of three basic machine learning paradigms, aims to learn an optimal or nearly optimal policy that maximizes the expected cumulative reward through exploration and exploitation [10]. Inspired both by the fields, we proposed PLUCB for P300-based BCI.

2.1 PLUCB algorithm

In accordance to the fundamental of multi-armed bandit problem [26,27], we model the problem of detecting P300 as a 2-armed bandit problem with context information. For each subject, a set of arms, $\mathcal{A} = \{a_p, a_n\}$, is given. The arms a_p and a_n both are indicators. Every time, PLUCB choose one from a_p and a_n according to its strategy. The choice is its judgement. The arm a_p represents that P300 is considered to exist in the EEG epoch and the arm a_n indicates that no P300 is considered to exist in the EEG epoch.

Formally, the algorithm PLUCB proceeds in discrete trials $t = 1, 2, 3, \cdots$. In trial t, PLUCB observes the context $e_t \in \mathbb{R}^d$, a d-dimensional feature vector summarizing the information of the current EEG epoch, evaluates a_p and a_n using e_t and its arm-selection strategy, and chooses an arm $a_t \in \mathcal{A}$. Here, the EEG epoch is considered to have P300 if $a_t = a_p$, or not if $a_t = a_n$. In a setting of copying experiment of P300 BCI, the experiment platform knows whether P300 exists in the EEG epoch or not. PLUCB can receive payoffs about its choice from the experiment platform.

Let $r_{t,p}$ and $r_{t,n}$ respectively be the payoffs of a_p and a_n in Trial t.

$$\begin{cases} r_{t,p} = 1, r_{t,n} = 0 & \text{if P300 exists} \\ r_{t,p} = 0, r_{t,n} = 1 & \text{otherwise} \end{cases} \tag{1}$$

After Trial t, PLUCB updates its arm-selection strategy with e_t, $r_{t,p}$ and $r_{t,n}$.

The total T-trial payoff is defined as $\sum_{t=1}^{T} r_{t,a_t}$, and the optimal expected T-trial payoff is defined as $\mathbf{E}[\sum_{t=1}^{T} r_{t,a_t^*}]$, where a_t^* is the arm with a maximum expected payoff in Trial t. Moreover, the T-trial regret of PLUCB can be defined by

$$R(T) \triangleq \mathbf{E}[\sum_{t=1}^{T} r_{t,a_t^*}] - \mathbf{E}[\sum_{t=1}^{T} r_{t,a_t}] \tag{2}$$

The goal of PLUCB is to minimize $R(T)$. We assume that the expected payoff of an arm a is linear in e_t with an unknown coefficient vector θ. For all t, we have

$$\mathbf{E}[r_{t,a}|e_t] = \theta_a^\top e_t,\ a \in \mathcal{A} \tag{3}$$

In trial t, let $D \in \mathbb{R}^{t\times d}, D = [e_1, e_2, \cdots, e_t]^\top$ represent the contexts of the t trials and $r_a = [r_{1,a}, r_{2,a}, \cdots, r_{t,a}]^\top$ for all $a \in \mathcal{A}$ indicate the payoffs of the t trials. Applying ridge regression [35] to $\{(D, r_a)|a \in \mathcal{A}\}$, the estimates of θ_a can be obtained as follows:

$$\hat{\theta}_a = (D^\top D + \mathbf{I}_d)^{-1} D^\top r_a,\ a \in \mathcal{A} \tag{4}$$

where $\mathbf{I}_d$ is a $d \times d$ identity matrix.

For simplicity, we use Φ to represent $D^\top D + \mathbf{I}_d$. When components in r_a are independently conditioned on corresponding rows in D, according to [36], we have:

$$|\mathbf{E}[r_{t+1,a}|e_{t+1}] - \hat{\theta}_a^\top e_{t+1}| \le \alpha\sqrt{e_{t+1}^\top \Phi^{-1} e_{t+1}},\ a \in \mathcal{A} \tag{5}$$

with the probability at least $1 - \delta$, where $\alpha = 1 + \sqrt{\ln(2/\delta)/2}$, both δ and α are constants. Eq. 5 gives a tight upper confidence bound for the expected payoff of arm a. From Eq. 5, we can derive an arm-selection strategy for Trial $t + 1$:

$$a_{t+1} = \arg\max_{a\in\mathcal{A}} \left(\hat{\theta}_a^\top e_{t+1} + \alpha\sqrt{e_{t+1}^\top \Phi^{-1} e_{t+1}}\right) \tag{6}$$

Based on the above fundamental, PLUCB, expressed as Algorithm 1, is proposed to implement calibration-free P300 BCI.

Algorithm 1 P300 linear upper confidence bound (PLUCB)

Input: $\alpha \in \mathbb{R}_+$
$\Phi \leftarrow \mathbf{I}_d$ (d-dimensional identity matrix)
$b_a \leftarrow \mathbf{0}_{d\times 1}$ (d-dimensional zero vector), $a \in \mathcal{A}$
for $t = 1, 2, 3, \cdots, T$ **do**
  observe the features $e_t \in \mathbb{R}^d$
  $\hat{\theta}_a \leftarrow \Phi^{-1} b_a$, $a \in \mathcal{A}$
  $p_{t,a} \leftarrow \hat{\theta}_a^\top e_t + \alpha\sqrt{e_t^\top \Phi^{-1} e_t}$, $a \in \mathcal{A}$
  $a_t = \arg\max_{a\in\mathcal{A}} p_{t,a}$
  output a_t as the decision for Trial t
  observe the payoffs $r_{t,a}$, $a \in \mathcal{A}$
  $\Phi \leftarrow \Phi + e_t e_t^\top$
  $b_a \leftarrow b_a + r_{t,a} e_t$, $a \in \mathcal{A}$
end for

2.2 TPLUCB algorithm

On a BCI platform where PLUCB is included, any person can use P300 BCI without having to calibrate it. PLUCB is based on the fundamental of reinforcement learning. When we consider this problem from the perspective of transfer learning, there is still room for improving this approach.

Suppose that N subjects, $\{S_i|i = 1, \cdots, N\}$, have used the PLUCB BCI platform before a new subject,

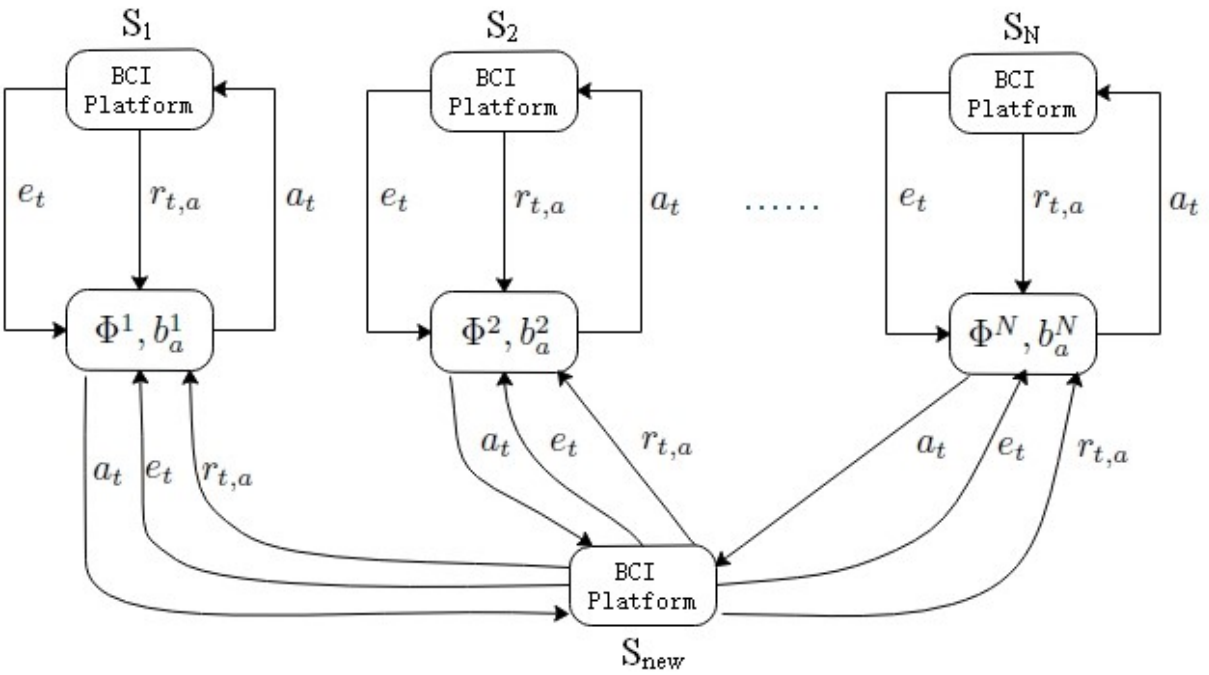

Fig. 1 The framework of TPLUCB. Before a new subject, S_{new}, comes, TPLUCB has obtained $\{\Phi^i, b_a^i | i = 1, \cdots, N,\ a \in \mathcal{A}\}$ by learning during the interactions with the source subjects $\{S_i | i = 1, \cdots, N\}$. TPLUCB starts running for S_{new} using $\{\Phi^i, b_a^i | i = 1, \cdots, N,\ a \in \mathcal{A}\}$ and keep improving the classification performance according to the feedbacks of the BCI platform.

S_{new}, comes. In the view of transfer learning [6–9], we have the source domain $\mathcal{D}_S = \{P(\mathbf{X}_a^i), D^i, r_a^i | i = 1, \cdots, N,\ a \in \mathcal{A}\}$, where, $\mathbf{X}_a^i$ is a random variable and indicates the situation of the feature vectors of S_i under the condition a, $P(\mathbf{X}_a^i)$ represents the probability distribution of $\mathbf{X}_a^i$, $D^i \in \mathbb{R}^{T \times d}$ is a matrix consisting of the d-dimensional vectors of S_i in T trials, r_a^i is a T-dimensional payoff vector of S_i in T trials under the condition a. Obviously, $\mathcal{D}_S$ is valuable for S_{new}. We further propose transferred PLUCB (TPLUCB) as described in Fig. 1.

The interactions between $\{\Phi^i, b_a^i\}$ and S_i in Fig. 1 show that, before S_{new} starts using the BCI platform, the algorithm TPLUCB has learned $P(\mathbf{X}_a^i)$ from (D^i, r_a^i) and obtained $\{\Phi^i, b_a^i\}$, the knowledge representation about $P(\mathbf{X}_a^i)$, for all i and a. All $\{\Phi^i, b_a^i\}$ can be viewed as a pool of predictors. The target domain can be described as $\mathcal{D}_T = \{P(\mathbf{X}_a^{new}), D^{new}, r_a^{new} | a \in \mathcal{A}\}$, where, $\mathbf{X}_a^{new}$ is a random variable and indicates the situation of the feature vectors of S_{new} under the condition a, $P(\mathbf{X}_a^{new})$ represents the probability distribution of $\mathbf{X}_a^{new}$, $D^{new} \in \mathbb{R}^{M \times d}$ is a matrix consisting of the d-dimensional vectors of S_i in M trials, r_a^{new} is a M-dimensional payoff vector of S_{new} in M trials under the condition a. In this study, D^{new} and r_a^{new} are null or have very small amount of data, we need to estimate the probability of a feature vector of S_{new} under condition a.

According to the fundamental of transfer learning [6–9] and our previous study [37], only a few source subjects share similar probability distribution with S_{new}. Formally, it can be expressed as $\{P(\mathbf{X}_a^i) \sim P(\mathbf{X}_a^{new}) | a \in \mathcal{A}, i \in \mathcal{N}, \mathcal{N} \subset \{1, \cdots, N\}, |\mathcal{N}| \ll N\}$, where $\sim$ means that the two probability distributions are similar.

As shown in Fig.1, TPLUCB has represented its knowledge on $P(\mathbf{X}_a^i)$ with $\{\Phi^i, b_a^i\}$ for all i and a. As shown in Eq. 5, when $\{\Phi^i, b_a^i\}$ is used to estimate the probability of a feature vector of S_i under condition a, there exists a tight upper confidence bound for the deviation of this estimate under a probability condition. Therefore, the arm-selection strategy, shown as Eq. 6, can be derived from the upper bound. The underlying logic is that, the larger the objective value in Eq. 6, the more likely this estimate is to be close to reality. When we seek the most appropriate knowledge from the source domain for the arm-selection strategy of S_{new}, this logic remains valid. So, the knowledge about $P(\mathbf{X}_a^i)$ can help S_{new} to start using P300 BCI when D^{new} and r_a^{new} are null.

After D^{new} and r_a^{new} begin to have data, TPLUCB exploits the feature vectors and payoffs from S_{new} to update the arm-selection strategy of S_{new}. The process

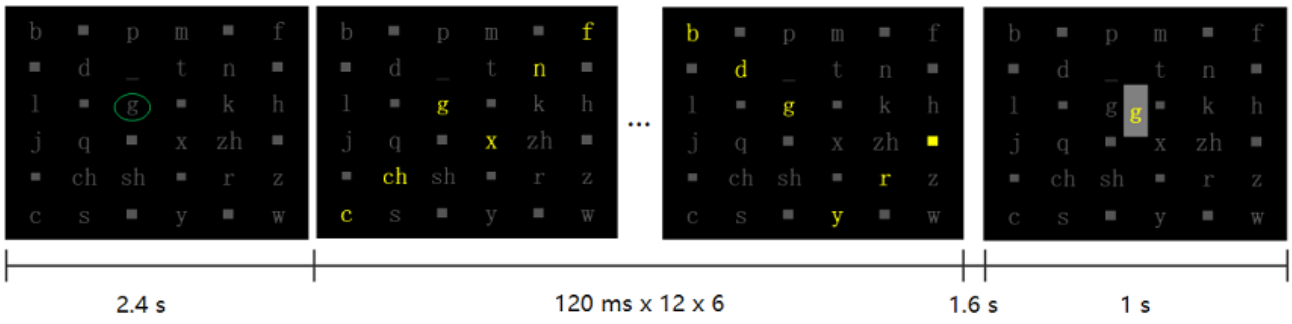

Fig. 2 Illustration of the symbol selection procedure on the BCI platform. This course includes 3 steps. Step 1 cues the current target for 2.4 s using an ellipse frame, as shown in the first screen. Step 2 contains six sequences of flashes. In each sequence, each of the 12 groups of symbols is flashed one time in a random order. Step 2 is shown in the section of the second screen to the third screen. The intensification of the flash lasts 80 ms and the interval between the successive intensification onsets is 120 ms. Step 2 lasts $120\,ms \times 12 \times 6 = 8640\,ms$ in total. Step 3 presents the result of symbol detection for 1s, as shown in the fourth screen.

is presented by the interactions between $\{\Phi^i, b_a^i\}$ and S_{new} in Fig.1. Compared to PLUCB, TPLUCB does not initiate $\{\Phi^i, b_a^i\}$ with the identity matrix and zero vector, but it starts with the knowledge learned from S_i. For S_{new}, the update does not change the probability basis of the arm-selection strategy, but its knowledge representation. So, Eq. 6 still applies. In summary, TPLUCB can be formally described as Algorithm 2, in which $i \in \{1, \cdots, N\}, a \in \mathcal{A}$.

Algorithm 2 Transferred P300 linear upper confidence bound (TPLUCB)

Input: $\alpha \in \mathbb{R}_+$
obtain $\{\Phi^i, b_a^i\}$ for all i and a through PLUCB
for $t = 1, 2, \cdots, T$ **do**
  observe the features $e_t \in \mathbb{R}^d$
  $\hat{\theta}_a^i \leftarrow (\Phi^i)^{-1} b_a^i$ for all i and a
  $p_{t,a}^i \leftarrow (\hat{\theta}_a^i)^\top e_t + \alpha\sqrt{e_t^\top (\Phi^i)^{-1} e_t}$ for all i and a
  $a_t = \arg\max_{a,i} p_{t,a}^i$
  output a_t as the decision for Trial t
  observe the payoffs $r_{t,a}$ for all a
  $\Phi^i \leftarrow \Phi^i + e_t e_t^\top$ for all i
  $b_a^i \leftarrow b_a^i + r_{t,a} e_t$ for all i and a
end for

3 Experiment and data

3.1 Experiment platform

Based on BCI2000 [28], we developed a P300 BCI platform that supports Chinese pinyin. In the BCI platform, a standard 6×6 matrix of symbols [25] is used to present stimuli according to checkerboard stimulus paradigm, which can reduce the errors caused by the flashes of non-target rows or columns that are adjacent to the target [38]. Before starting an experiment, the BCI platform randomly rearranges the 36 symbols in an inner matrix of 6×6. In a sequence, the BCI platform flashes the six groups of symbols in the presentation matrix corresponding to six rows of the inner matrix one time in a random order, then flashes six other groups of symbols in the presentation matrix corresponding to six columns of the inner matrix one time in a random order. The flash interfaces are shown in Fig. 2.

In the BCI platform, the number of sequences is configurable. The main characteristic of the BCI platform is that the symbols in the presentation matrices are not English characters but the symbols of Chinese pinyin, which are composed of the initial consonant, vowel or tone. The BCI platform supports subjects to successively select the initial consonant, vowel or tone of a Chinese character. Fig. 2 illustrates the procedure of selecting the initial consonant for a Chinese character. The procedures of selecting the vowel or tone for a Chinese character are similar.

3.2 Subjects

Twenty right-handed BCI-naive university students (10 males, 10 females) were recruited to participate in this study. They were at the age of 19 - 28 with the mean at 23 and the standard deviation at 2.35. The exclusion conditions include visual or neurological disorders, head trauma and any drug use that would affect nervous system function. Before the experiments, the subjects were asked to wash their hair. This experiment was approved by the Institutional Review Board at Fuzhou University (No. FZUBCI003, 8-Sep-2018). In accordance with the Helsinki Declaration of Human Rights, informed con-

sents for the experimentation were obtained from all subjects after a detailed explanation of the study.

3.3 Experiment paradigm

All subjects performed two sessions respectively at two different times. The first session used a pseudo-detector. That is, in the first session, the outcomes provided for the subjects were generated by the BCI platform according to the configured error rates, and the subjects were told that a real detector was working. Before the second session, a real classifier was trained on the data of the first session by SWLDA. In the second session, the classifier was used to detect P300 and the detection of the symbols was implemented by synthesizing a group of successive detections of P300. Each session included 14 runs. In each run, the subjects selected 18 symbols of Chinese pinyin. For each symbol, six sequences of flashes were presented. Every time a symbol was selected by the platform, it was presented to the subject.

A procedure of selecting a symbol on the BCI platform is illustrated in Fig. 2. It includes three steps. The first screen of Fig. 2 is Step 1, in which the current target is cued for 2.4s using an ellipse frame. Step 2 contains six sequences of flashes. In each sequence, each of the 12 groups of symbols is flashed once. There is no break in-between sequences. The intensification of the flash lasts 80 ms and the interval between the successive intensification onsets is 120 ms. The section of the second screen to the third screen in Fig. 2 presents Step 2, in which the subjects are instructed to silently count how many times the target has been flashed to keep their attention. The fourth screen in Fig. 2 represents Step 3, in which the result of symbol detection is presented.

3.4 EEG data

EEG signals were recorded by a 64-channel Neuroscan system, including the EEG cap, the amplifier, and the signal acquisition software. For convenience, we only recorded the EEG signals of 32 channels, which were: FP1 FP2 F7 F3 Fz F4 F8 FT7 FC3 FCz FC4 FT8 T7 C3 Cz C4 T8 TP7 CP3 CPz CP4 TP8 P7 P3 Pz P4 P8 PO7 PO8 O1 Oz O2. The sampling rate was set to 1000 Hz.

The raw EEG signals were firstly processed by common average reference and finite impulse response with the order at 64 and the frequency range of 0.5-30Hz. Here, each symbol selection underwent $12 \times 6 = 72$ flashes, and the 800 ms EEG signals following the flash onsets were processed for each flash. For brevity, we defined the onset moment of the first flash during a symbol selection as 0 ms. Every EEG segment from -300 ms to 9320 ms was cut out from the raw EEG signals.

Next, each EEG segment was normalized by subtracting the mean of -300 to 0 ms on each channel and dividing it by the median of standard deviations of all channels during -300 to 0 ms. Then, every 800 ms EEG epoch following a flash onset was extracted from the EEG segments and transformed into e_t, the 120-dimensional feature vector of trial t, by averaging every 40 ms on the channels of Fz, Cz, Pz, Oz, PO7 and PO8. Accordingly, $\{r_{t,a}|t = 1, \cdots, T, a \in \mathcal{A}\}$ were labelled in the light of the feedback of the BCI platform. For each subject, e_t and $r_{t,a}$ from Session 1 and Session 2 were gathered respectively into his/her training set and test set, in which $t = 1, \cdots, T$ is in the order of online experiment. The training sets were constructed after Session 1 and before Session 2, and were used only by SWLDA. The test sets were constructed after the two sessions, and were used in the simulated online experiments of PLUCB and TPLUCB.

3.5 Simulated online experiment

In this study, we used SWLDA, a frequently-used classifier in P300 BCI [28–31], as the baseline to evaluate the proposed PLUCB and TPLUCB. For SWLDA, the classifiers were calibrated on the training sets (from the first session) and applied in the corresponding second sessions, which are real online experiments. For PLUCB and TPLUCB, simulated online experiments were carried out directly on the test sets (from the second sessions) without any calibration on the training sets. We assess the performances of PLUCB and TPLUCB by comparing PLUCB and TPLUCB with SWLDA.

Without undergoing any calibration, PLUCB was directly applied to each test set. PLUCB proceeded in the order of $t = 1, 2, 3, \cdots, T$. After completing the testing of PLUCB on the 20 subjects, we had $\{\Phi^i, b^i_a|i = 1, \cdots, 20, a \in \mathcal{A}\}$ and went ahead to test TPLUCB. When the Ith subject was tested, we used $\{\Phi^i, b^i_a|i \in \mathcal{S}, \mathcal{S} = \{1, \cdots, 20\} - \{I\}, a \in \mathcal{A}\}$ as known knowledge from source subjects. Likewise, TPLUCB was directly applied to each test set without any calibration and proceeded in the order of $t = 1, 2, 3, \cdots, T$. A process of PLUCB or TPLUCB for each t is called a *round*.

In *Round* t_c, PLUCB and TPLUCB both updated their respective arm-selection strategies according to $r_{t_c,a}$ and e_{t_c}, and utilized the updated arm-selection strategy to process $\{e_t|t = t_c + 1, \cdots, T\}$ respectively. Let $N_{correct}$ and N_{all} respectively represent the numbers of the correctly classified e_t and all e_t in $\{e_t|t =$

$t_c+1,\cdots,T\}$, then $\frac{N_{correct}}{N_{all}}$ is called the *sample accuracy* of PLUCB or TPLUCB at *Round* t_c.

During the testing, every 72 successive sample classification results were synthesized into the result of detecting a symbol. Let $N'_{correct}$ and N'_{all} respectively represent the numbers of the correctly detected symbols and all symbols corresponding to $\{e_t|t=t_c+1,\cdots,T\}$, then $\frac{N'_{correct}}{N'_{all}}$ is called the *symbol accuracy* of PLUCB or TPLUCB at *Round* t_c.

For PLUCB, the way of synthesizing successive sample classification results to detect a symbol is described as follows. The first step is to compute ξ_r. $\xi_r=\sum_t(p_{t,a_p}-p_{t,a_n})$, where, $r\in\{1,\cdots,6\}$ indicates a row of the inner symbol matrix, $t\in\mathbb{T}_r$, $\mathbb{T}_r$ represents the set of the *round* numbers when the rth row symbols of the inner symbol matrix are flashed during the interaction for the current symbol, p_{t,a_p} and p_{t,a_n} are the results of the algorithm PLUCB at *Round* t. The second step is to calculate ξ_c, where $c\in\{1,\cdots,6\}$ represents a column of the inner symbol matrix, in a similar way to the first step. The final step is to determine the current symbol by $\hat{r}$ and $\hat{c}$, where $\hat{r}=\arg\max_r\xi_r$ and $\hat{c}=\arg\max_c\xi_c$.

For TPLUCB, the first and second steps of PLUCB synthesization are used to accumulate successive sample classification results of each source subject model. Let ξ_r^i and ξ_c^i represent the accumulated results of the model of the ith source subject, then the current symbol is determined by $\hat{r}$ and $\hat{c}$, where $\hat{r}=\arg\max_{r,i}\xi_r^i$ and $\hat{c}=\arg\max_{c,i}\xi_c^i$.

We tested PLUCB and TPLUCB in another way as well. PLUCB and TPLUCB only processed e_t when proceeding in the order of $t=1,2,3,\cdots,T$. After T *rounds*, the sample accuracy and symbol accuracy of PLUCB or TPLUCB on $\{e_t|t=1,\cdots,T\}$ of a subject were respectively called *overall sample accuracy* and *overall symbol accuracy* of PLUCB or TPLUCB on the subject. F-measure (F1) of PLUCB or TPLUCB on a subject is calculated by Eq. 7 [39]:

$$F1=\frac{2\times precision\times recall}{precision+recall} \tag{7}$$

where precision is the ratio of the number of the samples correctly classified as P300 to the number of the samples classified as P300, and recall is the ratio of the number of the samples correctly classified as P300 to the number of the P300 samples. Information transfer ratio (ITR) in bits/min is calculated by Eqs. 8 and 9 [40]:

$$B=\log_2 N+P\log_2 P+(1-P)\log_2[(1-P/(N-1))] \tag{8}$$

$$ITR=B\times(60/Dur) \tag{9}$$

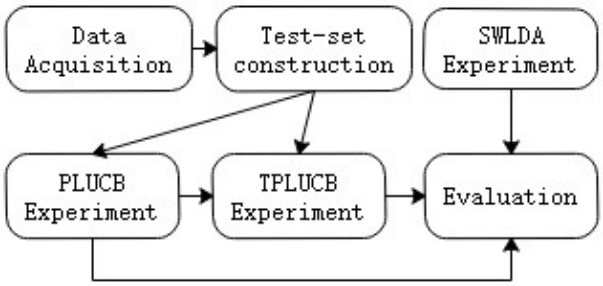

Fig. 3 Experimental block diagram

where N is the number of the symbols in the presentation matrix, P is the *overall symbol accuracy*, and Dur is the time (in second) needed to convey a symbol.

3.6 Overall experiment description

As shown in Fig. 3, the experimental work includes Data Acquisition, Test-set Construction, SWLDA Experiment, PLUCB Experiment, TPLUCB Experiment and Evaluation. The method of Data Acquisition is described in the sections of 3.1, 3.2, 3.3 and 3.4. The construction of training sets is included in Data Acquisition. The online SWLDA Experiment is conducted in the process of Data Acquisition. Following Data Acquisition, the procedures (Test-set Construction) described in the 3.4 section are conducted to generate the test sets. Subsequently, the simulated online experiments of PLUCB and TPLUCB (PLUCB Experiment and TPLUCB Experiment) are carried out on the test sets. Finally, PLUCB and TPLUCB are evaluated by the comparison with SWLDA (Evaluation). The methods of PLUCB Experiment, TPLUCB Experiment and Evaluation are described in the 3.5 section.

3.7 Statistical analysis

In the stage of Evaluation, t-test and analysis of variance (ANOVA) are used to assess PLUCB and TPLUCB. For the evolutions of PLUCB and TPLUCB, t-test is applied to compare the accuracies at each *round*. According to the principle of t-test, the normality of the relevant data sets is confirmed before each t-test. For each *round*, t-test is conducted four times to compare the *sample accuracies* of PLUCB on all subjects with those of SWLDA, the *symbol accuracies* of PLUCB on all subjects with those of SWLDA, the *sample accuracies* of TPLUCB on all subjects with those of SWLDA, and the *symbol accuracies* of TPLUCB on all subjects with those of SWLDA. For each t-test, the null hypothesis is that the means of the accuracies in the two groups

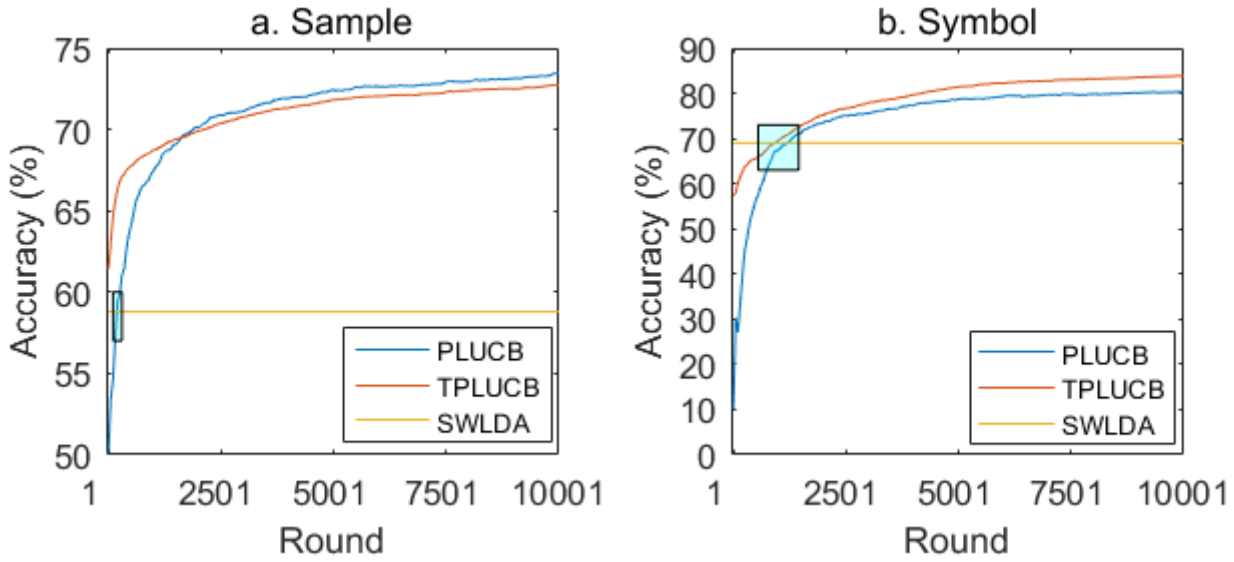

Fig. 4 Changes of the accuracies over *rounds*. A *round* means a process of PLUCB or TPLUCB for each t. In Figure (a), the 1-200 *rounds*, 201-400 *rounds* and 401-10000 *rounds* are called initial stage, tight stage and superior stage respectively. The tight stage is marked by the blue frame. The 'SWLDA' line represents the mean *sample accuracy* of SWLDA over 20 subjects (58.79%). The 'PLUCB' and 'TPLUCB' curves show the changes of the mean *sample accuracies* of PLUCB and TPLUCB over *rounds* respectively. In the initial stage, the mean *sample accuracy* of PLUCB is significantly lower than that of SWLDA, however it raises quickly. In the tight stage, the t-tests of the *sample accuracies* between PLUCB and SWLDA show no significant difference (p-value>0.05). In the superior stage, the mean *sample accuracies* of PLUCB are significantly higher than that of SWLDA. From *Round* 1, TPLUCB has higher mean *sample accuracies* than SWLDA. Its mean *sample accuracy* increases rapidly until *Round* 500. After *Round* 500, the mean *sample accuracy* of TPLUCB continues to improve at a slower rate. Before *Round* 1700, the mean *sample accuracy* of TPLUCB is higher than that of PLUCB. After *Round* 1700, the mean *sample accuracy* of TPLUCB is slightly lower than that of PLUCB. In Figure (b), the 1-750 *rounds*, 751-2100 *rounds* and 2101-10000 *rounds* are called initial stage, tight stage and superior stage respectively. The tight stage is also marked by the blue frame. The 'SWLDA' line is the mean *symbol accuracy* of SWLDA over 20 subjects (68.97%). The 'PLUCB' and 'TPLUCB' curves show the changes of the mean *symbol accuracies* of PLUCB and TPLUCB over *rounds* respectively. In the initial stage, the mean *symbol accuracy* of PLUCB is significantly lower than that of TPLUCB, the mean *symbol accuracies* of the two are significantly lower than that of SWLDA but both raise fast. In the tight stage, the t-tests of the *symbol accuracies* between PLUCB and SWLDA or between TPLUCB and SWLDA show no significant difference (p-value>0.05). In the superior stage, the mean *symbol accuracies* of PLUCB and TPLUCB are significantly higher than that of SWLDA and both continue to improve at slower rates, TPLUCB has a slight advantage over PLUCB in the *symbol accuracy*.

are equal, and the significant level is 0.05. Regarding the overall performances, ANOVA is employed to compare the *overall sample accuracies*, *overall symbol accuracies*, F-measures and ITRs of PLUCB, TPLUCB and SWLDA on all subjects. For each performance index, the null hypothesis of ANOVA is that the means of the performance values of PLUCB, TPLUCB and SWLDA are equal, and the significant level is 0.05. If the null hypothesis of ANOVA is rejected, Tukey-Kramer multiple-comparison is further used to detect the pairwise differences of PLUCB, TPLUCB and SWLDA.

4 Results

Fig. 4 presents the accuracies of SWLDA, PLUCB and TPLUCB. The 'SWLDA' lines exhibit the mean *sample accuracy* (in Fig. 4a) and the mean *symbol accuracy* (in Fig. 4b) of SWLDA on 20 subjects. The 'PLUCB' and 'TPLUCB' curves in Fig. 4a present the mean *sample accuracies* of PLUCB and TPLUCB respectively for all subjects at each *round*. Similarly, the 'PLUCB' and 'TPLUCB' curves in Fig. 4b respectively show the mean *symbol accuracies* of PLUCB and TPLUCB for all subjects at each *round*. Fig. 4 shows not only the accuracies of PLUCB, TPLUCB and SWLDA but also their changes and comparisons.

In Fig. 4a, the 1-200 *rounds*, 201-400 *rounds* and 401-10000 *rounds* are respectively called initial stage, tight stage and superior stage. In the initial stage, the *sample accuracies* of PLUCB are significantly lower than that of SWLDA. Fig. 5a presents an example of comparing PLUCB and TPLUCB with SWLDA in *sample accuracy* on each subject at *Round* 100 in the stage. In the tight stage, the t-tests of the *sample accuracies* between PLUCB and SWLDA show no significant difference (p-value>0.05). An example of comparing PLUCB

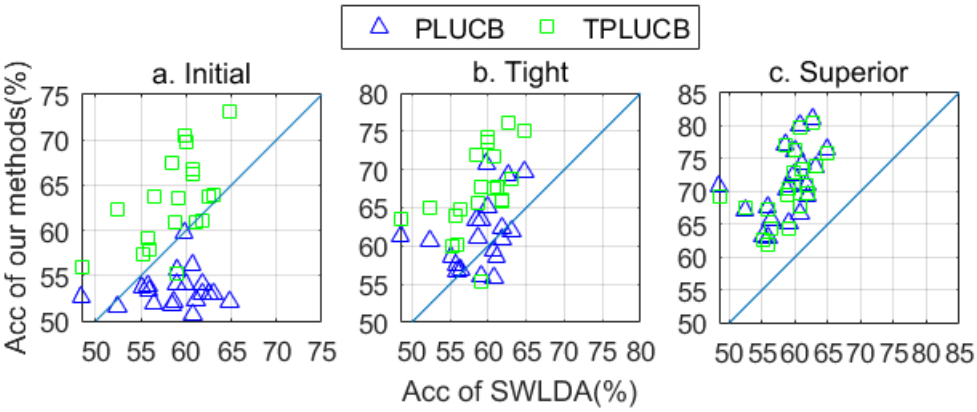

Fig. 5 Comparison of PLUCB and TPLUCB with SWLDA in *sample accuracy* on each subject. The Y axis represents the accuracy (Acc) of PLUCB (triangle points) or TPLUCB (square points), the X axis represents the accuracy (Acc) of SWLDA. Each triangle point represents the comparison on a subject between PLUCB and SWLDA and each square point represents the comparison on a subject between TPLUCB and SWLDA. Points above the diagonal line indicate that the accuracies of PLUCB or TPLUCB are higher than those of SWLDA for the subjects. Figure (a) shows the comparison of PLUCB and TPLUCB with SWLDA at *Round* 100 in the initial stage. At *Round* 100, the accuracies of PLUCB are clearly lower than those of SWLDA for most subjects, whereas the accuracies of TPLUCB are obviously higher than those of SWLDA. The comparison in Figure (b) is at *Round* 400 in the tight stage. At *Round* 400, TPLUCB still outperforms SWLDA in *sample accuracy* for most subjects, but PLUCB already has comparable *sample accuracy* with SWLDA for most subjects. In Figure (c), the comparison is at *Round* 3000 in the superior stage. At *Round* 3000, both of PLUCB and TPLUCB are clearly superior to SWLDA in *sample accuracy* for all subjects.

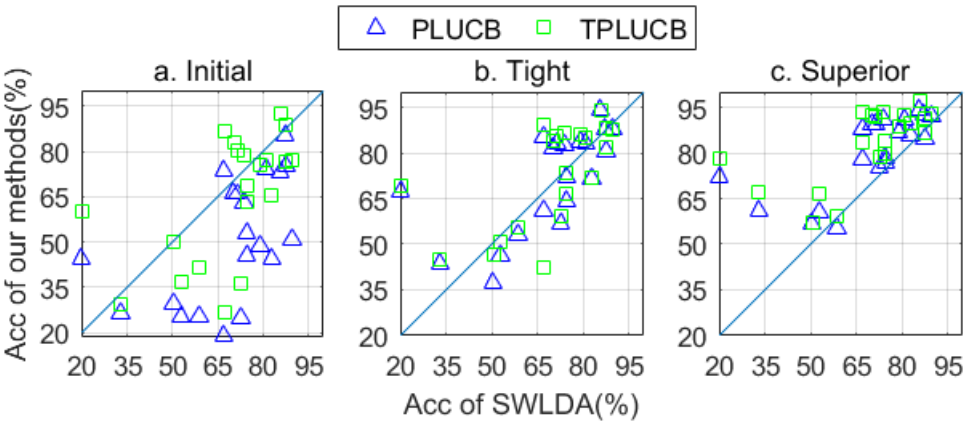

Fig. 6 Comparison of PLUCB and TPLUCB with SWLDA in *symbol accuracy* on each subject. This figure presents the comparisons in *symbol accuracy* in the same way as Fig. 5. The comparison of PLUCB and TPLUCB with SWLDA at *Round* 500 in the initial stage is shown in Figure (a), in which, for most subjects, the *symbol accuracies* of PLUCB and TPLUCB are lower than those of SWLDA. The comparison in Figure (b) is at *Round* 1500 in the tight stage. At *Round* 1500, no significant difference between PLUCB and SWLDA or between PLUCB and SWLDA in *symbol accuracy* is discovered for most subjects. In Figure (c), the comparison at *Round* 8500 in the superior stage is presented. At *Round* 8500, both PLUCB and TPLUCB are clearly superior to SWLDA in *symbol accuracy* for a majority of subjects.

and TPLUCB with SWLDA in *sample accuracy* on each subject at *Round* 400 in the stage is given in Fig. 5b. In the superior stage, the *sample accuracies* of PLUCB are significantly higher than that of SWLDA. An example of comparing PLUCB and TPLUCB with SWLDA in *sample accuracy* on each subject at *Round* 3000 in the stage is shown in Fig. 5c.

In Fig. 4b, the 1-750 *rounds*, 751-2100 *rounds* and 2101-10000 *rounds* are respectively called initial stage, tight stage and superior stage. In the initial stage, the *symbol accuracies* of PLUCB and TPLUCB are significantly lower than that of SWLDA. An example of comparing PLUCB and TPLUCB with SWLDA in *symbol accuracy* on each subject at *Round* 500 in the stage is given in Fig. 6a. In the tight stage, the t-tests of

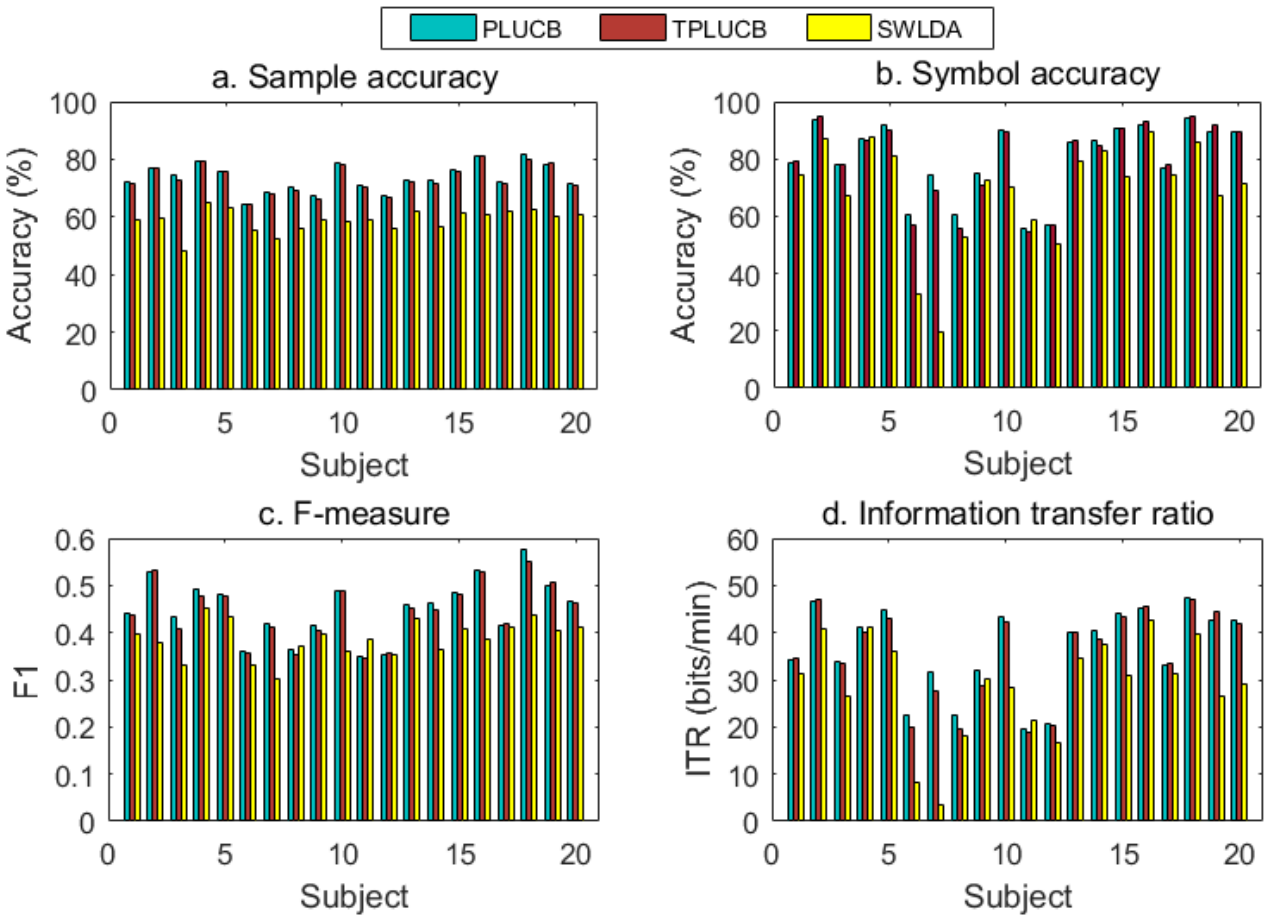

Fig. 7 Overall performance. The *overall sample accuracies*, *overall symbol accuracies*, F-measures and ITRs of PLUCB, TPLUCB and SWLDA on each subject are shown in Figure (a), (b), (c) and (d), respectively. In Figure (a), the *overall sample accuracies* of PLUCB and TPLUCB are obviously higher than those of SWLDA for all subjects. In Figure (b), the overall symbol accuracies of PLUCB and TPLUCB are higher than those of SWLDA for a majority of subjects. In Figure (c), both PLUCB and TPLUCB outperform SWLDA in F-measure for most subjects. In Figure (d), both PLUCB and TPLUCB outperform SWLDA in ITR for most subjects.

the *symbol accuracies* between PLUCB and SWLDA or between TPLUCB and SWLDA show no significant difference (p-value>0.05). Fig. 6b presents an example of comparing PLUCB and TPLUCB with SWLDA in symbol classification accuracy on each subject at *Round* 1500 in the stage. In the superior stage, the *symbol accuracies* of PLUCB and TPLUCB are significantly higher than that of SWLDA. An example of comparing PLUCB and TPLUCB with SWLDA in *symbol accuracy* on each subject at *Round* 8500 in the stage is shown in Fig. 6c.

Fig. 7 presents the four overall performance indices of the three methods in a histogram manner. Furthermore, for each one of the four overall performance indices, ANOVA was conducted on the performance values of PLUCB, TPLUCB and SWLDA on all subjects. The results of ANOVA show that, for all the four overall performance indices, there are significant differences among the three methods (p values<0.05). The following Tukey-Kramer multiple-comparison is presented in Table 1. As shown in Table 1, PLUCB and TPLUCB both significantly outperform SWLDA in *overall sample accuracy*, *overall symbol accuracy*, F1 and ITR, and no significant difference between PLUCB and TPLUCB is discovered for all the four overall performance indices.

5 Discussion

A true calibration-free approach, including the PLUCB and TPLUCB algorithms, is proposed in this study to implement P300-based BCI. Both PLUCB and TPLUCB allow a user to start using P300-based BCI without any calibration and can improve effectively in accordance with the feedbacks of the BCI platform during usage. The difference between PLUCB and TPLUCB lies in

Table 1 Multiple comparisons of the three methods. An empty entry represents that no significant difference is found between the two methods. According to the Tukey-Kramer multiple-comparison, the symbols ↑ and ↓ represent significantly higher and lower, respectively. The symbol entries are interpreted row-wise. For example, ↑ of (PLUCB,SWLDA) in Sub-table (a) means that the *overall sample accuracies* of PLUCB are significantly higher than those of SWLDA.

	PLUCB	TPLUCB	SWLDA
mean±std	73.6±4.8	73.1±4.9	58.8±3.8
PLUCB			↑
TPLUCB			↑

(a) *Overall sample accuracy*. The means and standard deviations of *overall sample accuracies* are shown in % for each method. The comparison results are represented by the symbols ↑ and ↓.

	PLUCB	TPLUCB	SWLDA
mean±std	80.4±12.8	79.6±14.0	69.0±18.3
PLUCB			↑
TPLUCB			↑

(b) *Overall symbol accuracy*. The means and standard deviations of *overall symbol accuracies* are shown in % for each method. The comparison results are indicated by the symbols ↑ and ↓.

	PLUCB	TPLUCB	SWLDA
mean±std	0.45±0.06	0.44±0.06	0.38±0.04
PLUCB			↑
TPLUCB			↑

(c) F-measure. The means and standard deviations of F-measures are shown for each method. The symbols ↑ and ↓ mean the comparison results.

	PLUCB	TPLUCB	SWLDA
mean±std	36.4±9.1	35.5±9.8	28.7±10.7
PLUCB			↑
TPLUCB			↑

(d) ITR. The means and standard deviations of ITRs are shown for each method. The symbols ↑ and ↓ show the comparison results.

that PLUCB does not have any priori knowledge but TPLUCB has some knowledge transferred from other persons when beginning working. Compared to the calibrated methods, the weakness of calibration-free approach lies in performance. In general, calibration-free approaches don't perform so well as calibrated methods, especially at the initial stage when calibration-free approaches have not sufficiently adapted to the subjects. The results presented in Figs. 4-6 show the strong adaptive capacity of the proposed approach.

From the perspective of *sample accuracy*, the case is as follows. PLUCB can achieve comparable performance with calibrated SWLDA by updating of only 200 *rounds*, continue to significantly improve by subsequent updating, and finally reach a very high mean *sample accuracy* that is almost 15% higher than that of SWLDA. TPLUCB has outperformed SWLDA from *Round* 1, can quickly increase the performance to a high point that is about 10% higher than that of SWLDA, and can maintain the trend of improvement while proceeding.

From the viewpoint of *symbol accuracy*, the situation can be described as follows. In the initial stage, PLUCB undergoes a process of adaption and TPLUCB's performance is slightly lower than that of SWLDA. PLUCB and TPLUCB can both work as well as SWLDA in the tight stage and significantly surpass SWLDA in the superior stage. The initial stage in the measurement of *symbol accuracy* is longer than that in the measurement of *sample accuracy*. The advantage of the proposed approach over SWLDA in the measurement of *symbol accuracy* is not so significant as that in the measurement of *sample accuracy*. We infer that the point was probably missed during synthesizing the successive sample classification results. Although this problem is not the core of the proposed approach, the integration of the successive sample classification results will obviously influence the performance of P300-based BCI. The observation actually implies a future direction of improvement for the proposed approach.

Figs. 4-6 mainly exhibit an observation of the performance trends of the proposed approach. Another observation of the proposed approach is presented in Fig. 7 and Table 1. The *overall sample accuracy*, *overall symbol accuracy*, F-measure and ITR in Fig. 7 and Table 1 all reflect the overall performance of the entire evolution of the proposed approach. The intuition from the graphical presentation in Fig. 7 is that PLUCB and TPLUCB both are superior to the SWLDA regardless of which one of the four overall performance indices is used. The further statistical analyses verify this intuition. Table 1 shows the multiple comparisons of the overall performances of PLUCB, TPLUCB and SWLDA.

In summary, the simulated online experiments have shown that the proposed approach not only allows starting P300-based BCI without any calibration, but also has significant performance advantages over SWLDA, a frequently-used method that needs calibration. The proposed approach is a very good option for the implementation of a P300-based BCI.

Regarding the comparison of PLUCB and TPLUCB, TPLUCB can adapt to a new subject more quickly than PLUCB, but no significant difference of overall performance is discovered between PLUCB and TPLUCB. On the one hand, the goal of TPLUCB is to speed up the adaption of PLUCB to new subjects. Compared to

this goal, TPLUCB is successful. On the other hand, we think that the initial advantage of TPLUCB over PLUCB is gradually attenuated during the evolutions and is not finally embodied by the overall performances.

Further work will be carried out to improve the study.

Firstly, the real online experiments will be carried out in the future. Since the judgement of TPLUCB depends on the competition among the models rather than the combination of the models, only a few models contribute to the judgement of TPLUCB after a period of running. Therefore, TPLUCB can be simplified in the real online environment.

Secondly, the proposed approach can be further improved. We can give several examples. The way of integrating successive sample classification results to detect a given symbol deserves further exploration. The detection of error-related potentials is expected to provide more natural feedbacks. As well, adjusting the assumption that the expected payoff of an arm a is linear in e_t probably leads to the emergence of a novel approach.

Finally, it is possible to extend the proposed approach to other EEG identification problems. There are two examples. We can conceive that a variation of this approach is applied to the detection of the intentions of users to spell or pause, which can help implement a flexible interaction in the context of P300-based BCI [41]. A new version of this approach can be used to detect event-related synchronization or desynchronization in motor imagery BCI. We will extend the proposed approach to new applications in future.

6 Conclusions

Although the prospect of BCI is very attractive, BCI has not been widely applied. The cost of calibration is one of the reasons. Inspired by the ideas of reinforcement learning and transfer learning, we proposed a calibration-free approach for P300-based BCI, which is able to learn during the usage by exploration and exploitation. The proposed approach includes two algorithms: PLUCB and TPLUCB. Both algorithms support the P300-based BCI to start working without any calibration. We assessed the performance trends and overall performances of the two algorithms through the simulated online experiments. The results show that both PLUCB and TPLUCB can quickly adapt to new users and have obvious advantages over SWLDA, a commonly-used method that needs calibration, in the overall performances. In summary, the proposed approach can be used to implement calibration-free P300-based BCI.

Acknowledgment

Zhilei Lv, Faqiang Peng and Ting Li participated in this work when they studied at Fuzhou University. We thank them for their contributions.

Compliance with Ethical Standards

Funding: This study was supported by the Transformation Project of Scientific and technological achievements of Fuzhou, China (2020-GX-12) and Natural Science Foundation of Fujian Province,China (2019J01242). Conflict of Interest: No conflict of interest exists. Ethical approval: All procedures performed in the study involving human participants were in accordance with the ethical standards of the Institutional Review Board at Fuzhou University and with the 1964 Helsinki declaration and its later amendments. Informed consent: Informed consent was obtained from all individual participants included in the study.

References

1. J. R. Wolpaw, E. W. Wolpaw (Eds.), Brain-Computer Interfaces: Principles and Practice, Oxford University Press, New York, USA, 2012.
2. B. J. Edelman, J. Meng, D. Suma, C. Zurn, E. Nagarajan, B. S. Baxter, C. C. Cline, B. He, Noninvasive neuroimaging enhances continuous neural tracking for device control, Science Robotics 4 (31) (2019) eaaw6844.
3. P. K. Shukla, R. K. Chaurasiya, S. Verma, Performance improvement of P300-based home appliances control classification using convolution neural network, Biomedical Signal Processing and Control 63 (2021) 102220.
4. R. Bauer, A. Gharabaghi, Reinforcement learning for adaptive threshold control of restorative brain-computer interfaces: a bayesian simulation, Frontiers in neuroscience 9 (2015) Article 36.
5. R. Abiri, S. Borhani, E. W. Sellers, Y. Jiang, X. Zhao, A comprehensive review of EEG-based brain–computer interface paradigms, Journal of Neural Engineering 16 (1) (2019) 011001.
6. S. Ben-David, J. Blitzer, K. Crammer, A. Kulesza, F. Pereira, J. W. Vaughan, A theory of learning from different domains, Machine Learning 79 (1-2) (2010) 151–175.
7. S. J. Pan, Q. Yang, A survey on transfer learning, IEEE Transactions on Knowledge and Data Engineering 22 (10) (2010) 1345–1359.
8. V. Jayaram, M. Alamgir, Y. Altun, B. Scholkopf, M. Grosse-Wentrup, Transfer learning in brain-computer interfaces, IEEE Computational Intelligence Magazine 11 (1) (2016) 20–31.
9. Z. Wan, R. Yang, M. Huang, N. Zeng, X. Liu, A review on transfer learning in EEG signal analysis, Neurocomputing 421 (2021) 1–14.
10. L. P. Kaelbling, M. L. Littman, A. W. Moore, Reinforcement learning: A survey, Journal of Artificial Intelligence Research 4 (1996) 237–285.

11. K. Crammer, O. Dekel, S. Shalev-Shwartz, Y. Singer, Online passive-aggressive algorithms, Journal of Machine Learning Research 7 (3) (2006) 551–585.
12. E. Hazan, Introduction to online convex optimization, Foundations and Trends in Optimization 2 (3-4) (2015) 157–325.
13. S. Fazli, F. Popescu, M. Danóczy, B. Blankertz, K.-R. Müller, C. Grozea, Subject-independent mental state classification in single trials, Neural Networks 22 (9) (2009) 1305–1312.
14. P.-J. Kindermans, M. Tangermann, K.-R. Müller, B. Schrauwen, Integrating dynamic stopping, transfer learning and language models in an adaptive zero-training ERP speller, Journal of Neural Engineering 11 (3) (2014) 035005.
15. N. T. Gayraud, A. Rakotomamonjy, M. Clerc, Optimal transport applied to transfer learning for p300 detection, in: BCI 2017-7th Graz Brain-Computer Interface Conference, 2017, p. 6.
16. H. Qi, Y. Xue, L. Xu, Y. Cao, X. Jiao, A speedy calibration method using riemannian geometry measurement and other-subject samples on a P300 speller, IEEE Transactions on Neural Systems and Rehabilitation Engineering 26 (3) (2018) 602–608.
17. D. Hübner, P.-J. Kindermans, T. Verhoeven, K.-R. Müller, M. Tangermann, Rethinking BCI paradigm and machine learning algorithm as a symbiosis: Zero calibration, guaranteed convergence and high decoding performance, in: Brain-Computer Interface Research, Springer, 2019, pp. 63–73.
18. J. Lee, K. Won, M. Kwon, S. C. Jun, M. Ahn, CNN with large data achieves true zero-training in online P300 brain-computer interface, IEEE Access 8 (2020) 74385–74400.
19. F. Li, Y. Xia, F. Wang, D. Zhang, X. Li, F. He, Transfer learning algorithm of P300-EEG signal based on xdawn spatial filter and riemannian geometry classifier, Applied Sciences 10 (5) (2020) 1804.
20. A. Buttfield, P. W. Ferrez, J. R. Millan, Towards a robust BCI: error potentials and online learning, IEEE Transactions on Neural Systems and Rehabilitation Engineering 14 (2) (2006) 164–168.
21. P.-J. Kindermans, M. Schreuder, B. Schrauwen, K.-R. Müller, M. Tangermann, True zero-training brain-computer interfacing–an online study, PloS One 9 (7) (2014) e102504.
22. J. Grizou, I. Iturrate, L. Montesano, P.-Y. Oudeyer, M. Lopes, Calibration-Free BCI Based Control, in: Twenty-Eighth AAAI Conference on Artificial Intelligence, Quebec, Canada, 2014, pp. 1–8.
23. W. Liu, L. Zhang, D. Tao, J. Cheng, Reinforcement online learning for emotion prediction by using physiological signals, Pattern Recognition Letters 107 (2018) 123–130.
24. Z. Ma, J. Cheng, D. Tao, Online learning using projections onto shrinkage closed balls for adaptive brain-computer interface, Pattern Recognition 97 (2020) 107017.
25. L. A. Farwell, E. Donchin, Talking off the top of your head : toward a mental prosthesis utilizing event-related brain potentials, Electroencephalography and Clinical Neurophysiology 70 (6) (1988) 510–523.
26. L. Li, W. Chu, J. Langford, R. E. Schapire, A contextual-bandit approach to personalized news article recommendation, in: Proceedings of the 19th international conference on World wide web, 2010, pp. 661–670.
27. S. K. Kim, E. A. Kirchner, A. Stefes, F. Kirchner, Intrinsic interactive reinforcement learning–using error-related potentials for real world human-robot interaction, Scientific reports 7 (2017) 17562.
28. G. Schalk, D. J. McFarland, T. Hinterberger, N. Birbaumer, J. R. Wolpaw, BCI2000: a general-purpose brain-computer interface (BCI) system, IEEE Transactions on Biomedical Engineering 51 (6) (2004) 1034–1043.
29. F. Lotte, L. Bougrain, A. Cichocki, M. Clerc, M. Congedo, A. Rakotomamonjy, F. Yger, A review of classification algorithms for EEG-based brain-computer interfaces: a 10 year update, Journal of Neural Engineering 15 (3) (2018) 031005.
30. M. Arvaneh, I. H. Robertson, T. E. Ward, A P300-based brain-computer interface for improving attention, Frontiers in Human Neuroscience 12 (2019) 524.
31. B. Z. Allison, A. Kübler, J. Jin, 30+ years of P300 brain–computer interfaces, Psychophysiology 57 (7) (2020) e13569.
32. A. G. E. Collins, Reinforcement learning: bringing together computation and cognition, Current Opinion in Behavioral Sciences 29 (2019) 63–68.
33. E. J. Lawrence, L. Su, G. J. Barker, N. Medford, J. Dalton, S. Williams, N. Birbaumer, R. Veit, S. Ranganatha, J. Bodurka, Self-regulation of the anterior insula: Reinforcement learning using real-time fMRI neurofeedback, Neuroimage 88 (2014) 113–124.
34. A. Cortese, H. Lau, M. Kawato, Unconscious reinforcement learning of hidden brain states supported by confidence, Nature Communications 11 (2020) 4429.
35. A. E. Hoerl, R. W. Kennard, Ridge regression: Biased estimation for nonorthogonal problems, Technometrics 42 (1) (2000) 80–86.
36. T. J. Walsh, I. Szita, C. Diuk, M. L. Littman, Exploring compact reinforcement-learning representations with linear regression, arXiv preprint arXiv:1205.2606 (2012).
37. Z. Huang, W. Zheng, Y. Wu, Y. Wang, Ensemble or pool: A comprehensive study on transfer learning for c-VEP BCI during interpersonal interaction, Journal of Neuroscience Methods 343 (4) (2020) 108855.
38. G. Townsend, B. LaPallo, C. Boulay, D. Krusienski, G. Frye, C. Hauser, N. Schwartz, T. Vaughan, J. Wolpaw, E. Sellers, A novel P300-based brain-computer interface stimulus presentation paradigm: Moving beyond rows and columns, Clinical Neurophysiology 121 (7) (2010) 1109–1120.
39. T. Fawcett, An introduction to roc analysis, Pattern Recognition Letters 27 (8) (2006) 861–874.
40. P. Yuan, X. Gao, B. Allison, Y. Wang, G. Bin, S. Gao, A study of the existing problems of estimating the information transfer rate in online brain-computer interfaces, Journal of Neural Engineering 10 (2) (2013) 026014.
41. J. Mladenovic, J. Frey, M. Joffily, E. Maby, F. Lotte, J. Mattout, Active inference as a unifying, generic and adaptive framework for a P300-based BCI, Journal of Neural Engineering 17 (1) (2020) 016054.